Kinetic Studies on Cocoa Roasting Including Volatile Characterization

Rojas, Myriam; Osorio, Jessi; Heeres, Hero Jan; Chejne, Farid

Published in:
ACS Food Science and Technology

DOI:
10.1021/acsfoodscitech.1c00481

Publication date:
2022

ACS FOOD SCIENCE & TECHNOLOGY

pubs.acs.org/acsfoodscitech

Article

Kinetic Studies on Cocoa Roasting Including Volatile Characterization

Myriam Rojas, Jessi Osorio, Hero Jan Heeres, and Farid Chejne*

Cite This: *ACS Food Sci. Technol.* 2022, 2, 1224−1236

Read Online

ACCESS | Metrics & More | Article Recommendations

ABSTRACT: Despite roasting being the most crucial step in cocoa manufacture, its thermochemical effects on cocoa are not entirely understood. This work aims to understand the kinetics and chemical composition of the volatile compounds formed during roasting. The weight loss of two sizes of cacao powder was evaluated in thermogravimetric analysis (TGA) with five heating rates (10 to 180 °C min^{-1}), using air and nitrogen as the carrier gas. A global Friedman isokinetic model was used to obtain kinetic data from the TGA measurements. For this, seven different stages were discriminated, and the kinetics were determined for each stage separately. PTV−GC−MS identified the gas phase, and SPME−GC−MS quantified the volatile compounds trapped in the solid phase. At intermediate temperatures (150 to 250 °C), aromatics (e.g., pyrazines, aldehydes, ketones, phenols, and pyrroles) are formed and transferred to the gas at higher temperatures for a prolonged time. Typical Maillard and Strecker degradation reaction products in both gas and solid phases were identified and used to set up a reaction network for cocoa roasting.

KEYWORDS: *cacao, roasting, flavor, kinetics, Friedman model, volatilization*

INTRODUCTION

Thermal processing is well-known in the food industry (e.g., coffee, cacao, cereal) to obtain consumer products with desirable organoleptic characteristics. Chocolate is one of the most marketable products and has been used since ancient times. Chocolate was mainly used for nutritional purposes, though the demand for fine chocolate and its derivatives has increased dramatically.[1]

The final product quality of chocolate is defined by its flavor and aroma determined by the cacao genotype and the process of transforming cocoa to chocolate.[2] Although each stage of the processing is important regarding product properties, roasting is a crucial stage because here, the flavor and aroma of the cocoa are developed.[3] Roasting consists of heating the cacao beans at elevated temperatures until the beans are "cracking", but before they start to burn.[4] The roasting temperatures used are usually between 110 and 160 °C for 10 to 120 min. The term "cacao" refers to raw beans before roasting and "cocoa" is used for the beans after roasting.[5]

The roasting process causes major changes in cacao, such as fat-melting, drying, loss of volatile compounds flavor, denaturation of proteins, and darkening. Besides changes in the physical structure (e.g., reduced density), major changes in the chemical composition of the beans take place by a wide range of chemical reactions such as denaturation of proteins and lipid oxidation. Some of these reactions are preferred regarding product properties, some are undesired. Several relevant reactions and their effects on product properties, and particularly aroma and flavor development will be discussed below.

The Maillard reaction is considered one of the most relevant reactions during roasting,[6] and involves the condensation of free amino acids with reducing sugars of the cocoa presented in Table 1. Besides, other reactions such as Strecker degradation to produce Strecker-aldehydes and pyrazines occur in parallel and series.[7] The latter are considered important constituents and give the roasted cocoa, and the chocolate derived from it, a pleasant aroma.[8,9] It has been established that high sugar contents in the beans lead to fruity and floral flavor notes,[10] and a threshold value of 2590 mg kg^{-1} for fructose and 850 for glucose is proposed to obtain good product quality in terms of aroma and flavor.[11]

Cacao beans contain significant amounts of polyphenols (Table 1), and these are considered beneficial when regarding product properties related to positive health effects. As such, the roasting process should be tuned to preserve these polyphenols flavor.[8,12] However, under specific roasting conditions, these may degrade into undesirable compounds that are harmful to humans.[13]

Because of the high lipid content of cocoa (see Table 1), lipid oxidation reactions cannot be avoided, and result in usually undesirable compounds.[14] Examples are the formation of carbonyl compounds,[15] alcohols, and small organic acids.[16] Particularly, the latter is not preferred. An example of an undesired carbonyl compound is malonaldehyde (MDA), a genotoxic that may lead to mutations and subsequently to cancer.[17]

Received: December 30, 2021
Revised: March 11, 2022
Accepted: March 16, 2022
Published: April 14, 2022

https://doi.org/10.1021/acsfoodscitech.1c00481
ACS Food Sci. Technol. 2022, 2, 1224−1236

Table 1. Main Chemical Components of Raw Cocoa (Fermented and Dried)

main components	p/p % dry weight	ref
moisture content	6.5−7	18,19,20
total sugars	1.46−2.71	
total lipids content	32−57	
Lipids		
rac-1(3)-palmitoyl-3(1)-stearoyl-2-oleoyl glycerol (POSt)	49.6	21,22
1,3-distearoyl-2-oleoylglycerol (StOSt)	29.8	
2-oleo-dipalmitin (POP)	20.6	
proteins	15.5−17.9	14
Maillard precursors	mg/kg	ref
reducing sugars	10.8 ± 0.19	23
aspartic acid	0.64 ± 0.02	
asparagine	1.61 ± 0.07	
glutamic acid	1.81 ± 0.09	
leucine	3.33 ± 0.14	
alanine	2.44 ± 0.09	
phenylalanine	2.45 ± 0.04	
tyrosine	1.64 ± 0.05	
valine	1.34 ± 0.08	
isoleucine	0.98 ± 0.03	
tryptophan	1.34 ± 0.03	
lysine	2.48 ± 0.04	
serine	0.89 ± 0.04	
glycine	0.50 ± 0.01	
arginine	2.33 ± 0.07	
threonine	0.60 ± 0.02	
natural products	mg/g degreased cacao	ref
total polyphenols	33.55−71.66	24
theobromine	20.8−25.6	
caffeine	3.2−4.3	

Most studies in the field have focused on studying the effect of relevant process parameters for the roasting process (temperature and residence time) on product quality (i.e., pleasant flavor and aroma, Sacchetti et al., 2016;[25] Rojas et al., 2020;[19] Afoakwa et al., 2008;[9] Aprotosoaie et al., 2016[8]). However, these studies have not evaluated heating rates, inert roaster atmospheres, and particle sizes.

For a better understanding of the roasting process (process-product relations), improved technology development, and scale-up purposes, kinetic studies are inevitable. Kinetic studies reported in the literature so far on cocoa roasting (see Table 2) have mainly focused on the rate of moisture loss, the formation rate of 2,5-diketopiperazines (DKP) responsible for the bitter taste, rates of polyphenols degradation, color changes (i.e., darkening), HMF, melanoidins, and inactivation of *Stearothermophilu* spores. Also, Beidaghy et al.[26] using thermogravimetric analysis (TGA) at 10 °C min^{-1} and a first-order kinetic model, determined the average pyrolysis rate (dm/dt) as a criterion to measure the explosiveness of pulverized materials, where the cocoa powder was the least explosive with the lowest mean pyrolysis rate of 0.5 $\mu g/s$, compared to wheat flour and sugar with around 0.9 $\mu g/s$. However, the kinetic studies mentioned in Table 2 were carried out on bulk scale (beans) where there are diffusive and convective phenomena mixed, that is, outside the kinetic control scale, so the nature of the chemical reactions is still missing. Therefore, this research is pioneering because the experimentation was performed under a kinetically controlled scale (very small particles) and focused on nonisothermal kinetics to understand the thermal conversion of cocoa during roasting using isokinetic models, guaranteeing very reliable results.

Table 2. Kinetic Models Used in the Cocoa Roasting Process

variable	model	ref
moisture loss rate	Newton	
	Page	
	Henderson and Pabis	27
	two-term model	28
	Verma	29
	Peleg	25
	approximation of diffusion	
	Arrhenius	
2,5-diketopiperazines (DKPs) formation rate	zero-order and solid-state reaction	30
rate of polyphenol degradation	Weibull probabilistic cumulative	31
color lightness and hue angle changes	first and zero-order	25
HMF formation rate	exponential	25
Melanoidins generation rate	asymptotic	
Stearothermophilu spores inactivation	nonlinear cumulative Weibull distribution	32

In this work, TGA studies were performed on cocoa using different heating rates, and the effects of particle size and the carrier gas type (nitrogen, oxygen) on kinetics were established. The Friedman isokinetic model, recommended by Berčič[33] was applied together with the Osawa/Flynn/Wall (FWO), also known as ASTM E1641.[34] Both were successfully used to describe the TGA kinetics of biomass torrefaction and pyrolysis.[35] Besides, the volatiles formed at different temperature stages of the roasting process were determined qualitatively and quantitatively using a programmable temperature vaporizer injector coupled to gas chromatography with mass detector (PTV−GC−MS), and the volatiles present in the residue after roasting were quantified using solid-phase microextraction followed by GC analyses (SPME−GC−MS). In this way, the novelty of this work was to describe the thermal conversion of cocoa in a three-stage kinetic scheme and to propose a novel experimental strategy combining three analytical technologies (TGA, PTV−GC−MS, and SPME−GC−MS) able to describe the dynamics of weight loss and identify the chemical compounds generated in the solid phase and for the first time identify the compounds that are released into the gas phase during heating. In addition, a reaction network was proposed to explain the volatiles formed during the cocoa roasting under nonisothermal conditions joining the Maillard, Strecker degradation, and lipid oxidation reactions.

MATERIALS AND METHODS

Raw Material Characterization. In an electric blade grinder mill, samples of dry non-defatted fermented Colombian fine cocoa (*Criollo* variety from the municipality of Tumaco (latitude, 1.70417; longitude, −78.6953)) were frozen in liquid nitrogen and ground cryogenically to avoid crushing the plant structure (Hamilton Beach 80350R). The resulting powder was sieved, and subsequent studies were carried out with two particle sizes: small particles (<0.149 mm No. 100 U.S. Sieve) and large particles (<0.420 mm No. 40 U.S. Sieve) denoted S and L, respectively.

Moisture Content Determination (X_w). The moisture content of the cocoa beans was determined in triplicate using a Mettler Toledo HC103 moister analyzer with an accuracy of 0.0001 g at 105 °C. The average value is provided.

https://doi.org/10.1021/acsfoodscitech.1c00481
ACS Food Sci. Technol. 2022, 2, 1224−1236

Particle Size Distribution and Specific Surface Area. A Mastersizer[36] equipped with an automated Aero S dry powder disperser cell was used to determine the two cocoa bean samples' particle size distribution, specific surface area, and uniformity (size particle distribution spread). A dispersion pressure of 0.2 bar was used, the measurement duration was 10 s, and a particle refractive of 1.52 and an absorption index of 0.5 were assumed. The determinations were carried out five-times. The data provided are the average of all measurements.

Sugar Extraction and Quantification. One gram of sample was mixed with 5 mL of Milli-Q water intensively (vortex mixer) for 60 s at 70 °C. This was followed by an ultrasound treatment for 15 min at 40 Hz. The resulting slurry was centrifuged at 10 000 rpm for 15 min, and the supernatant was collected. The extraction procedure was repeated three times for the residue after centrifugation; the combined supernatants were filtered (0.22 mm nylon) before high-performance liquid chromatography (HPLC) injection. HPLC quantification was performed by the method described by Abdilla-Santes et al.[37] For this purpose, an Agilent 1200 series instrument was used, equipped with a Bio-Rad organic acid column (Aminex HPX-87 H, 60 °C), a refractive index (IR), and an ultraviolet detector (UV). The mobile phase consisted of aqueous sulfuric acid (5 mol m^{-3}) which was fed at a flow rate of 0.75 mL min^{-1}. An injection volume of 10 μL was applied. Calibration curves ($R^2 \geq 0.98$) were made with standards of maltose (99%, Sigma-Aldrich), glucose (99%, Sigma-Aldrich), and fructose (98%, Sigma-Aldrich) in the concentration range between 2.5 to 40 mg L^{-1}.

Thermogravimetric Analysis. TGA analyses were performed using the cocoa bean samples (1−2 mg) on a thermobalance TGA 4000 PerkinElmer (U.S.), using heating rates of 10 (β_1), 30 (β_2), 60 (β_3), 120 (β_4), and 180 °C min^{-1} (β_5) from 40 to 700 °C. Either nitrogen or air was used at a flow rate of 18 mL min^{-1}. Besides, a standard of TMP (pyrazine tetramethyl ≥ 98%, Sigma-Aldrich) was analyzed at a heating rate of 10 °C min^{-1} (β_1). Each analysis was done in duplicate and the relative standard deviation percentage (%RSD) was determined.

Gas-Phase Characterization. A programmable temperature vaporizing injector (PTV), model Optic 2 (Atlas) coupled to an HP 5890 GC Series II system equipped with a Restek 5Sil MS column (30 m × 0.25 mm i.d. × 0.1 μm) and an HP 5972 MS detector (PTV-GC−MS) controlled by an Optic 2 was used to analyze the volatiles of the gas-phase. Samples of cocoa powder were introduced into a 60 μL μ-vial that is placed inside the PTV injector liner and purged with helium to remove any air between the sample particles. The PTV allows controlling the heating rate and temperature as well as cooling with airflow. All the gases generated during the heating are injected directly into the GC−MS column, identifying the compounds released (gas phase) during the cocoa roasting. The heating rate was set at 120 °C min^{-1} (β_4), from 40 °C to a predetermined temperature (100, 125, 150, 175, 200, 250, 300, and 350 °C), with samples ranging from 5 to 15 mg, the exact amount depending on the signal of the volatiles in the mass detector. The following GC oven program was used: 1 min at 40 °C, then heating to 120 °C at 4 °C min^{-1}, to 180 °C at 5 °C min^{-1}, and to 310 °C at 10 °C min^{-1}, and then isothermal at 310 °C for 2 min. A split mode injection was done (ratio 1:50), and helium was used as the carrier gas at a flow rate of 1 mL min^{-1} The MS detector was operated in the scan range of m/z 30−500 using the electron ionization mode (70 eV) with an interface temperature of 280 °C. Volatile compounds were identified using the NIST05a mass spectra library.

Solid-Phase Characterization. It was done through SPME−GC−MS using the same chromatograph described in the previous step. Each solid residue after a PTV measurement was collected, weighed, and placed in a 10 mL HS vial containing a carboxy/polydimethylsiloxane (CAR/PDMS) fiber, preactivated at 280 °C for 30 min. The volatiles were adsorbed for 50 min at 60 °C and then desorbed from the fiber in the injector at 260 °C for 6 min using a SPME fiber holder with manual sampling and injection (Supelco, Italy) in splitless mode. The GC oven was programed as follows: 2 min at 40 °C, heating to 180 °C at 5 °C min^{-1}, then to 310 at 10 °C min^{-1}, and then isothermal at 310 °C for 2 min. The detection was in scan mode from 40 to 500 m/z, and the carrier gas, flow, ionization, and mass spectra library were the same as in the previous step.

Data Analyses and Kinetic Modeling. The thermogravimetric curves were smoothed by the Lowess method (span: 0.07) and used to investigate the nonisothermal kinetics during the heating of the cocoa powder. So, the Fourier deconvolution was applied to each *DTG* curve to filter the signal and separate the stages in peaks by a nonlinear adjustment model[38] using Matlab 2020a version. In this way, Friedman and ASTM E1641[34] isokinetic models were applied for global analysis (i.e., entire curve), and Friedman model for each separate stage (i.e., same peaks grouped). Thus, peak 1 corresponds to the first reaction (drying), and the following peaks to subsequent volatilization reactions. This work focused on analyzing the first four peaks (until 350 °C) and establishing a relationship with the identification of volatile compounds in PTV-GC.

The isoconventional Friedman model assumes that the rate of reaction ($d\alpha/dt$) at a constant conversion (α) is only a function of temperature and under nonisothermal conditions $d\alpha/dt$ is equal to eq 1, with a constant rate of heating β.

$$\frac{d\alpha_{(T)}}{dT} = \frac{A}{\beta} \exp^{-E_a/RT} f(\alpha_{(T)}) \tag{1}$$

$$\beta = \frac{dT}{dt} \tag{2}$$

$$T = T_0 + \beta_{(t)} \tag{3}$$

The temperature changes linearly with time as eq 2 and eq 3, where T_0 is the initial temperature, A is the pre-exponential factor, and E_a is the activation energy in J mol^{-1}, R is the universal gas constant (8.314 J/mol K), T is the absolute temperature at time t (in Kelvin and seconds, respectively), and α is given in eq 6. The logarithmic form of eq 1 is as eq 4, and for a given value of α is eq 5.

$$\ln\left(\frac{d\alpha_{(T)}}{dT}\beta\right) = -\frac{E_a}{RT} + \ln[Af(\alpha_{(T)})] \tag{4}$$

$$Af(\alpha_{(T)}) = C_{\text{constant}} \tag{5}$$

Graphically, the activation energy is obtained from the slope in a plot of $\ln\left(\frac{d\alpha}{dt}\right)$ vs $1/T$. To track the solid, we can use the conversion term alpha (α):

$$\alpha = \frac{m_0 - m(T)}{m_0 - m_f} \tag{6}$$

The Friedman model applied to each stage i, divided in groups of same peaks obtained by Fourier deconvolution is eq 7.

$$\frac{d\alpha_{i,(T)}}{dT} = \frac{A_i}{\beta} \exp^{-E_{ai}/RT} f(\alpha_{i,(t)}) \tag{7}$$

The α_i values for each stage were adjusted from 0 to 1 because each stage was analyzed as a separated and independent reaction, then the conversion was assumed complete at that specific stage.

RESULTS AND DISCUSSION

Cocoa Bean Characterization. The properties of the powder samples were determined, such as the moisture content, particle size distribution, and sugar content, which is a critical product property when considering flavor and aroma development during roasting. The cocoa beans were ground and sieved in two fractions (S and L) to determine particle size effects on the TGA kinetics. The cocoa bean samples had an average moisture percentage of 6.35 ± 0.02% wt. The particle sizes resulted in a bimodal distribution, where the S particles presented the largest amount around 40 μm and a second group around 90 μm, while the L particles showed a small group around 25 μm and a great group between 150 and 500 μm (Figure 1). This large group is likely due to some aggregation

https://doi.org/10.1021/acsfoodscitech.1c00481
ACS Food Sci. Technol. 2022, 2, 1224−1236

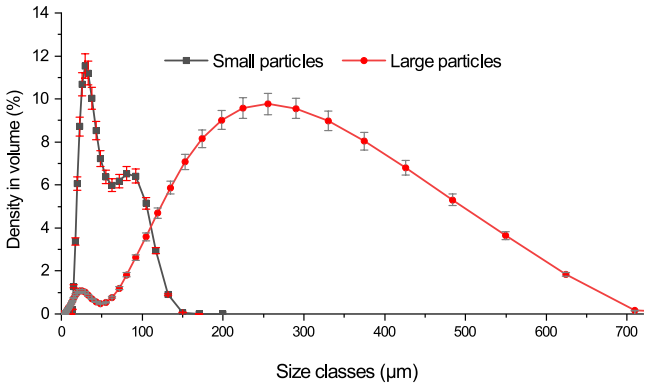

Figure 1. Particle size distribution of cocoa powder for small and large particles measured by laser diffraction particle sizing (Mastersizer 3000).

during collection and storage. In addition, a uniformity of 0.54 and 0.619 and a specific surface area of 20.90 ± 1.26 and 11.67 ± 0.68 $m^2\ kg^{-1}$ were determined for S and L, respectively.

The values of glucose and fructose were 2.78 and 5.07 mg g^{-1} d.b., respectively; both values were somewhat higher than that reported in the literature obtained by two extractions with constant stirring for 20 min but without ultrasound. For instance, values from 0.38 to 1.75 mg g^{-1} for glucose and 0.48 to 0.863 mg g^{-1} for fructose were reported for samples from Ecuador,[39] while examples from Brazil were reported to contain 1.93 mg g^{-1} of glucose, and the highest content of fructose of 5.94 mg g^{-1}.[40] Also, the samples had 2.35 mg g^{-1} of maltose and met the sugar content standards established by Araujo et al.[11] to produce the right amount of aromatics in the roasting process.

Thermogravimetric Analysis. A typical TGA curve for cocoa beans (sample S) in the air is showed in Figure 2. Several

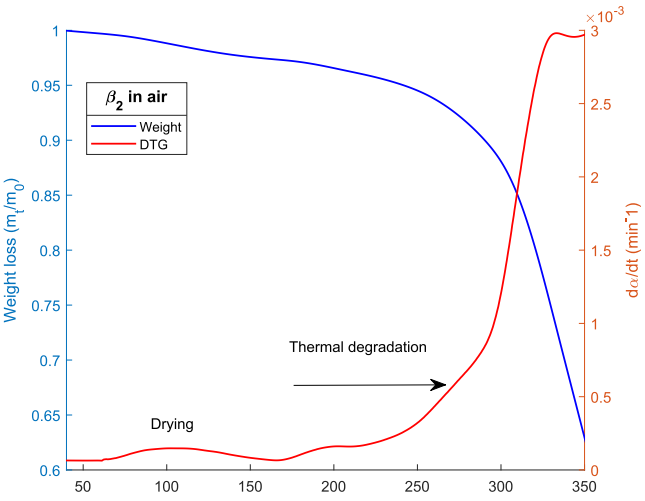

Figure 2. TGA curves of weight loss and DTG for cocoa beans (sample S, air, 30 °C min^{-1}).

stages are observed in the DTG as a result of different physical and chemical phenomena during roasting. The first stage at a maximum of 101 °C is associated with water removal and the release of low molecular weight chemical compounds. At 200 °C, a second stage is observed, which involves the volatilization of reaction products, for example, the Maillard reaction, Strecker degradation, and lipid oxidation.

In Table 3 and Figure 3 the weight loss between L and S particles did not significantly differ with N_2, while the air sample showed differences. The highest weight loss percentage occurred using air with a more significant difference after 300 °C (Figure 3c,d). When the air was used, the S particles lost weight faster up to 10.49%, while L particles only lost 4.35% at

Table 3. Comparison of the Final Weight Obtained in Thermogravimetric Analysis Using Air and Nitrogen as Carrier Gas[a]

carrier gas	% RSD in nitrogen TG curve		% RSD in air TG curve	
heating rate(°C/min)	S	L	S	L
10	2.14	1.55	1.01	1.07
30	1.05	0.80	1.81	1.83
60	0.53	1.65	2.32	3.14
120	0.52	4.19	2.11	4.69
180	1.04	1.03	1.82	3.03

final weight difference percentage between N_2 and air for the same particles size ($W_{air} - W_{N_2}$)

	S				L			
heating rate(°C/min)	250 °C	300 °C	350 °C	600 °C	250 °C	300 °C	350 °C	600 °C
10	0.84	10.49	25.53	2.45	0.53	4.35	14.39	5.13
30	0.26	1.58	16.69	14.46	1.21	1.53	7.63	12.91
60	0.21	0.76	3.81	17.66	0.50	0.43	0.18	10.35
120	0.09	0.13	0.81	12.20	0.57	0.53	0.46	5.16
180	0.23	0.02	0.30	5.56	0.55	0.53	0.42	0.30

final weight difference percentage between large and small particles for the same carrier gas ($W_L - W_S$)

	nitrogen				air			
heating rate(°C/min)	250 °C	300 °C	350 °C	600 °C	250 °C	300 °C	350 °C	600 °C
10	1.14	−0.13	2.50	3.53	0.22	6.02	13.65	0.85
30	0.24	0.62	1.25	0.27	0.72	0.67	10.31	1.82
60	0.78	0.75	0.79	1.53	0.08	0.44	2.84	5.78
120	0.60	0.75	1.06	1.15	0.13	0.09	0.20	5.89
180	0.24	0.57	0.54	1.63	0.08	0.02	0.18	4.23

[a]Final weight difference percentage (W) using air and N_2 as carrier gas. Relative standard deviation percentage (%RSD).

https://doi.org/10.1021/acsfoodscitech.1c00481
ACS Food Sci. Technol. 2022, 2, 1224−1236

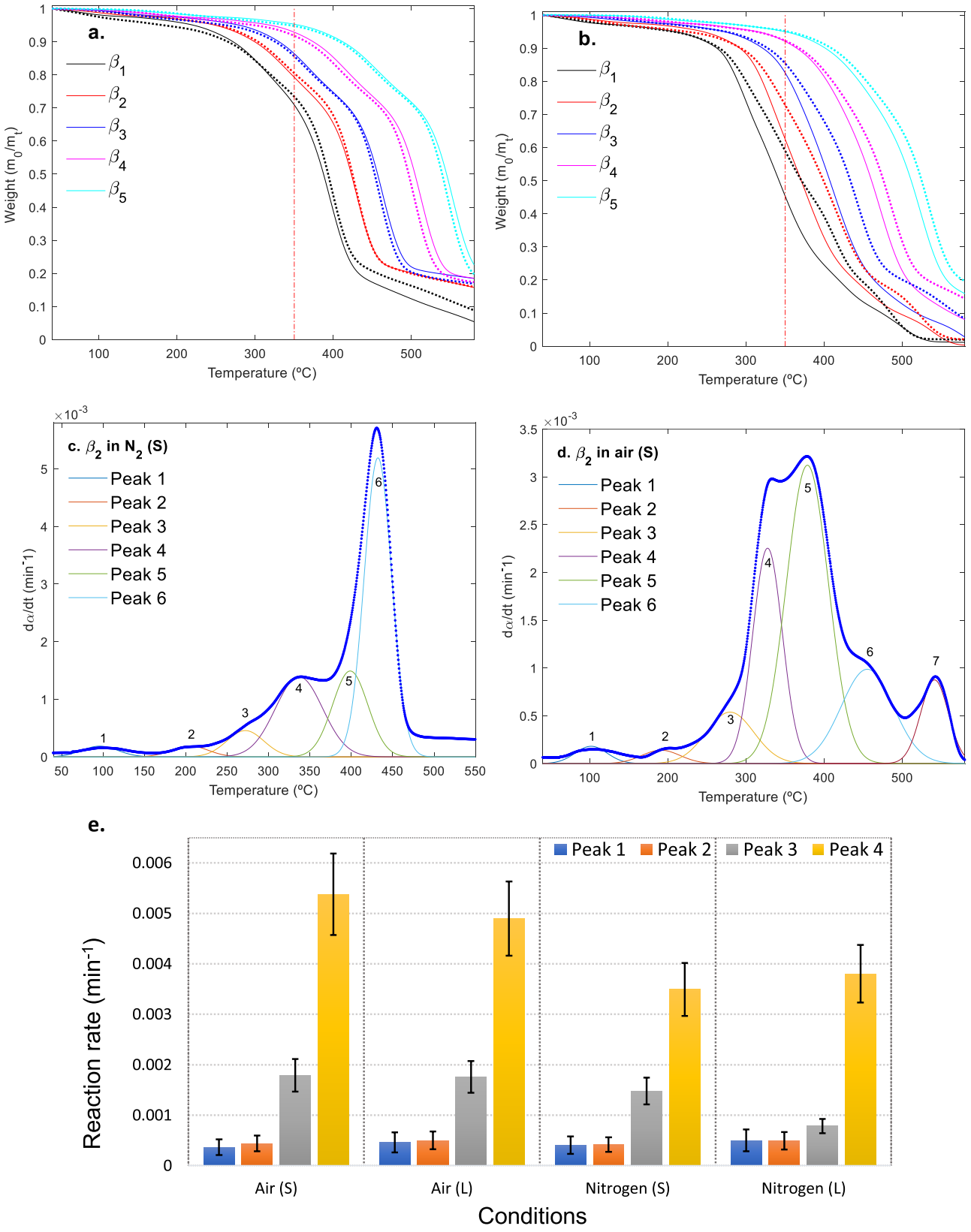

Figure 3. Curves of weight loss using a carrier gas of (a) nitrogen and (b) air for which dashed lines are large (L) particles and continuous lines are small particles (S). Fourier deconvolution of DTG curves for small particles with (c) N_2 and (d) air as carrier and (e) maximum reaction rates.

the same temperature of 300 °C (see Figure 3a,b). This effect is because S particles have a larger specific surface area than L, available for interaction between cocoa lipids and oxygen, causing lipid degradation reactions,[41] and this degradation accelerates volatilization measured in weight loss.

By Fourier deconvolution, we found six Gaussian peaks in the nitrogen curves (Figure 3a) and seven peaks for the air (Figure

https://doi.org/10.1021/acsfoodscitech.1c00481
ACS Food Sci. Technol. 2022, 2, 1224−1236

Table 4. Compounds Identified in the Gas Phase during Heating of Cocoa Powder by PTV-GC-MS at β_4[a]

Group	Component	Peak 1 <150°C	Peak 2 >150°C	Peak 3 ≤250°C	Peak 4 <350°C
CO_2	Carbon dioxide				
Acids	Acetic acid				
	Hexadecanoic acid				
	Octadecanoic acid				
Alcohols	1,3-Butanediol				
	2,3-Butanediol				
	Isopropyl Alcohol				
	Phenylethyl Alcohol				
Aldehydes	Butanal, 3-methyl-				
	2-Furancarboxaldehyde				
	2-Furancarboxaldehyde, 5-methyl-				
	Benzeneacetaldehyde				
Alkaloids	Theobromine				
	Caffeine				
Furans	2-Furanmethanol				
	2,5-Furandione, dihydro-3-methylene-				
	Furancarboxylic acid, methyl ester				
Ketones	2-Propanone, 1-hydroxy-				
	2-Butanone, 3-hydroxy-				
	2-Propanone, 1-(acetyloxy)-				
	2-Hydroxycyclopent-2-en-1-one				
	2-Cyclopenten-1-one, 3-methyl-				
	3-Methylcyclopentane-1,2-dione				
Ketones	3-Ethyl-2-hydroxy-2-cyclopenten-1-one				
Phenols	Phenol				
	Phenol, 4-methyl-				
	Phenol, 2-methoxy-				
	1,2-Benzenediol				
	1,2-Benzenediol, 4-methyl-				
Pyrroles	Pyrrole				
	Ethanone, 1-(1H-pyrrol-2-yl)-				
	Maltol				
	2,5-Pyrrolidinedione				
	3-Hydroxy-2,3-dihydromaltol				
	Indole				
	1H-Indole, 5-methyl-				
Pyrazines	Pyrazine, 2,5-dimethyl-				
	Pyrazine, trimethyl-				
	Pyrazine, 3-ethyl-2,5-dimethyl-				
	Pyrazine, tetramethyl-				
	Pyrazine, 2,5-dimethyl-3-(3-methylbutyl)-				
Others	Styrene				
	4(1H)-Pyridinone				
	3-Pyridinol				
	1,3-Diazine				
	Pyridine, 3-phenyl-				

[a]Supplemental Data is in Gas_data.dat.

Table 5. Activation Energies and Pre-exponential Factors Obtained for Global (with Friedman and ASTM) and Stages (Deconvolution Peaks by Friedman)[a]

	Small Sample				Large Sample			
peak	E_a	$A_i(n=0)$	$A_i(n=1)$	R^2	E_a	$A_i(n=0)$	$A_i(n=1)$	R^2
				Nitrogen Carrier Gas				
1	32.9 ± 0.05	108.1	216.2	0.98	34.2	906	1813	0.96
2	44.0 ± 0.08	449.1	889.4	0.99	48.6	1609	3218	0.98
3	47.8 ± 0.04	219.2	433.5	0.97	55.2	1674	3348	0.98
4	69.4 ± 0.06	5715	11430	0.96	64.7	2511	5023	0.97
5	75.0 ± 0.05	5634	71238	0.98	69.3	3594	7189	0.99
6	87.9 ± 0.1	28983	57966	0.98	90.2	46224	92448	0.96
Global Friedman	82.8 ± 0.11	6602	13204	0.96	88.7	20008	40017	0.95
Global ASTM	73.5 ± 0.12	2624	5248	0.97	79.0	4117	8234	0.95
				Air Carrier Gas				
1	31.6 ± 0.07	562.7	1125	0.97	32.4	191.7	383.5	0.96
2	38.5 ± 0.12	157.0	314.0	0.96	38.8	2294	4588	0.98
3	43.7 ± 0.09	99.4	198.8	0.98	46.6	153.7	307.5	0.97
4	50.3 ± 0.07	210.4	420.7	0.95	50.1	147.7	294.4	0.96
5	73.2 ± 0.05	4784	8969	0.96	72.1	3296	6592	0.98
6	110.2 ± 0.04	423723	907447	0.98	81.2	6195	12390	0.97
7	136.8 ± 0.13	5938486	11876973	0.97	125.9	1563935	3127871	0.96
Global Friedman	72.6 ± 0.16	1987	3974	0.95	95.7	65297	130559	0.97
Global ASTM	55.76 ± 0.21	961.9	1923	0.94	68.86	2294	4588	0.95

[a]Activation Energy in kJ/mol and pre-exponential factors (A_i) for reaction order n equals 0 and 1.

3b). For all cases, the adjustments resulted in R^2 greater than 0.98 and in reproducible results. There are more significant differences between N_2 and air peaks at lower heating rates β_1 and β_2. Figure 3 shows that the maximum average reaction rates were lower and similar in the first two peaks (101 and 200 °C) while increased in the peaks 3 and 4, where the highest rates were given by oxidant carrier gas, evidencing an accelerating effect on cocoa thermal degradation at temperatures hotter than 250 °C. Each peak was associated with a family of volatile compounds that are described later.

A typical displacement in weight loss curves is observed and, therefore, in the peaks resulting from the deconvolution. This displacement is due to the effect known as thermal lag, given by the thermal resistance that opposes the crucible and the sample since the temperature is measured at a point between the furnace and the crucible and not directly on the sample. Thus, the actual

https://doi.org/10.1021/acsfoodscitech.1c00481
ACS Food Sci. Technol. 2022, 2, 1224−1236

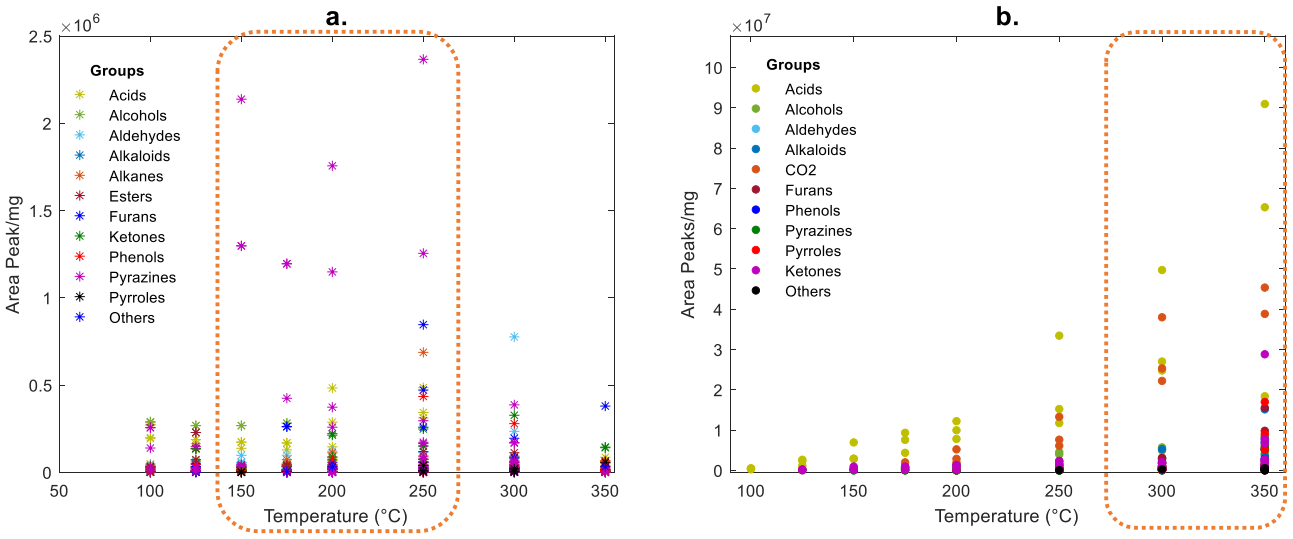

Figure 4. Comparison between compounds identified during the heating (a) in the solid phase and (b) in the gas phase.

sample temperature is slightly lower than that of the oven. This difference is larger when using higher heating rates.[42]

Chemical Compounds Identified in the Gas and Solid Phases. By PTV−GC−MS analysis of the gas phase and SPME−GC−MS of the solid phase, a great variation in the number and species of volatile compounds was determined at each temperature. The compounds identified in peak 1 (until 150 °C), were acetic acid, 2-propanone, 1-hydroxy, 2-butanone, 3 -hydroxy, 1,3-butanediol, and 2,3-butanediol (see Table 4). These compounds are products of the aerobic and anaerobic fermentation process of the cocoa beans before roasting.

The second peak is between 150 and 200 °C due to the loss of chemical water mass, the same volatile compounds as in peak 1, and some products of chemical reactions such as carbon dioxide aldehydes, pyrazines, pyrroles, theobromine, and caffeine (see Table 5). Furthermore, it was found that the largest number of compounds remaining in the solid phase was from 175 to 250 °C, with 30 and 27 volatile compounds, while just 7 to 15 compounds were volatilized. At 200 and 250 °C the greatest number of pyrazines (4) was found in the solid, along with aldehydes, esters, and some acids (see Figure 4). Pyrazines and aldehydes were also volatilized at 250 °C in the gas phase; that is, under these conditions, the aromatic compounds were formed within the solid by heating, but the temperature and time were enough to start to volatilize them toward the gaseous phase. The pyrazine tetramethyl (TMP) disappeared from the solid at 300 °C but remained in the gas phase until 350 °C.

The release of CO_2 and the presence of heterocyclic compounds from 175 °C is evidence of the Maillard reaction between reducing sugars and amino acids in the raw material. This follows the mechanism of degradation of Strecker proposed by Ruan et al.,[43] where Strecker aldehydes and pyrazines are generated that contribute significantly to the aroma of chocolate, which were identified in the solid and gas phases. Considering the results shown in Figure 4 since it is intended that pleasant aromatics are generated and that they remain within the solid, the range of temperature recommended is from 150 to 250 °C. At this temperature range there is an increase in the number of pyrazines because after 250 °C the pyrazines begin to volatilize to the gas. The pyrazines are critical to obtaining the pleasing aroma of roasted cocoa, providing up to 40% of that desirable characteristic. They are found in greater numbers and higher concentrations in fine cocoa beans from *Criollo*.[44] In addition, the number of components in the gas phase identified at 300 °C was 30 and increased to 44 at 350 °C; these components represent the signals of peaks 3 and 4 that are identified previously in the Fourier deconvolution.

Since the DTG profiles showed a faster volatilization rate in air, evidencing the predominance of different decomposition pathways, the acceleration of volatilization is attributed to the lipid oxidation reactions in the cocoa particles. In the same way, it has been detected that from the interaction of lipids with oxygen, lipids are transformed into molecules with new functional groups named lipid carbonyls because these reactive carbonyls may behave like carbonyls derived from carbohydrates and be able to react with the nucleophilic amino groups of amino acids to produce an analogous cascade of reactions traditionally considered exclusive to the Maillard reaction and generate the same Strecker products.[45] Therefore, to study these thermochemical processes on complex systems such as cocoa, which contain carbohydrates, lipids, and amino acids, both the Maillard and the oxidation of lipids reactions were considered to understand the chemical reactions and products directly related to the cocoa quality. Then, according to information from the literature of model systems[7] and the compounds identified in this work, the reactions network of Figure 5 was established.

The volatilization of Strecker degradation products such as aldehydes and pyrazines from 175 °C was identified, increasing the number and peaks area at higher temperatures, together with other intermediate products of the Maillard reaction such as furans, ketones, and pyrroles, evidencing the presence of different reaction pathways (Figure 5a). Aldehydes, pyrazines, furans, phenols, esters, and acids among other volatiles trapped within the solid, were also identified after heating (Figure 4). These groups of compounds were found in roasted cacao (*Criollo* variety from Peru) as a result of the same chemical reactions. However, the authors used traditional roasting under an isothermal mode (110−140 °C for 20−35 min), using a similar SPME methodology. However, the process was made on a bulk scale (kilograms of cocoa beans that are not under kinetic control). In addition, monitoring volatile compounds released into the gas phase during the process was not shown (Valle-Epquín et al., 2020).

https://doi.org/10.1021/acsfoodscitech.1c00481
ACS Food Sci. Technol. 2022, 2, 1224−1236

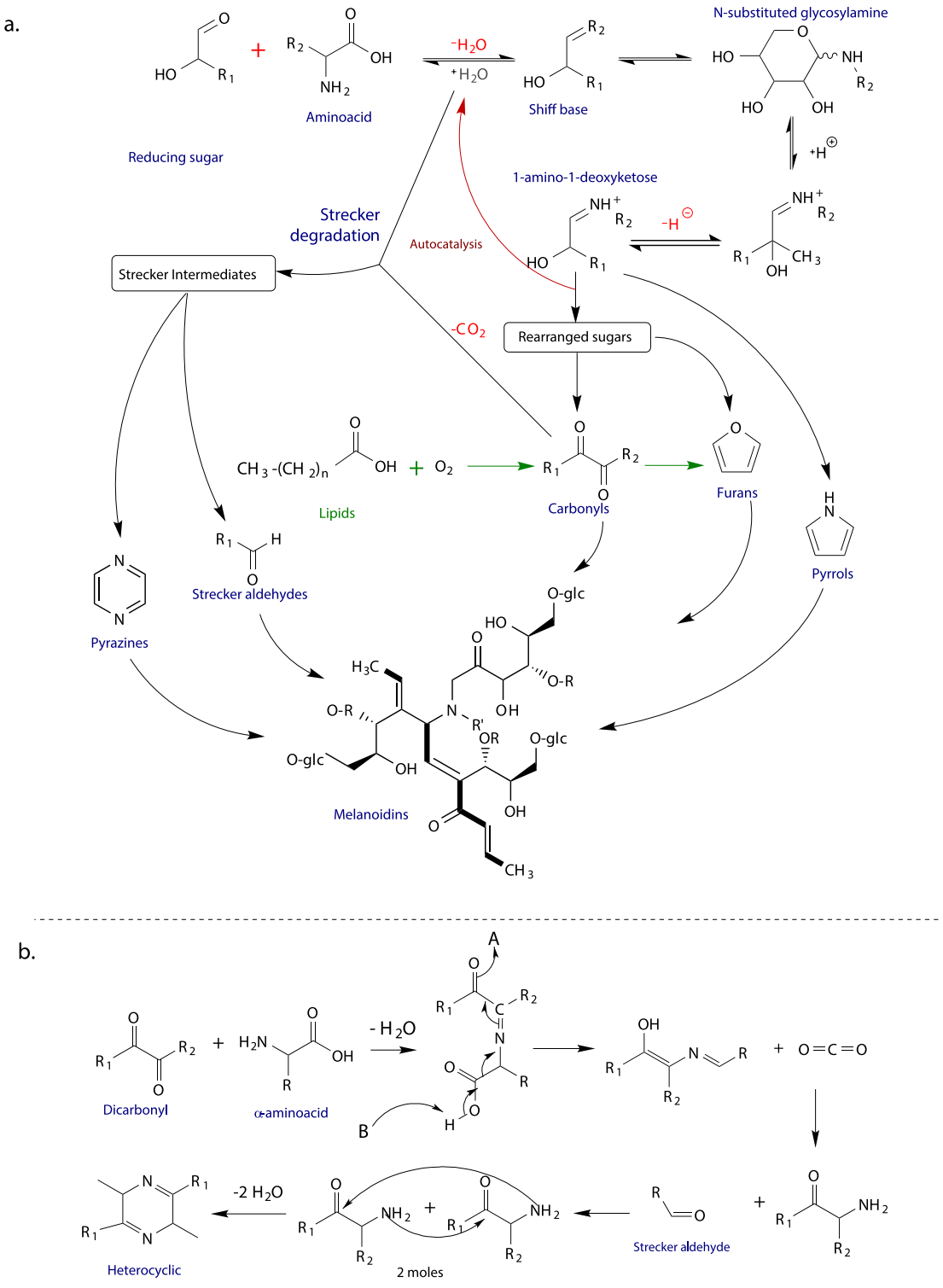

Figure 5. (a) Simplified reaction network for flavor generation by the Maillard reaction during cocoa roasting with the lipid oxidation pathway and (b) Strecker degradation mechanism.

$$(P_1)C \xrightarrow{K_1} D + W$$

$$(P_2)\,D \xrightarrow{K_2} R + V_1$$

$$(P_{3\,\&\,4})\,R \xrightarrow{K_3} O + V_2$$

Figure 6. Kinetic scheme in three stages where P_1 to P_4 mean peak 1 to peak 4 obtained by Fourier deconvolution.

The above is evidence that chemical reactions occur in the solid due to heating, and volatiles are produced. At low and intermediate temperatures these volatiles remain trapped within the solid phase, but when the temperatures and time increase, they are transferred to the gas phase. Besides, some of these intermediates may react with the reagents present; there are also autocatalytic reactions.[46] Therefore, considering that the quality of roasted cocoa is directly related to the aroma, knowing the

https://doi.org/10.1021/acsfoodscitech.1c00481
ACS Food Sci. Technol. 2022, 2, 1224−1236

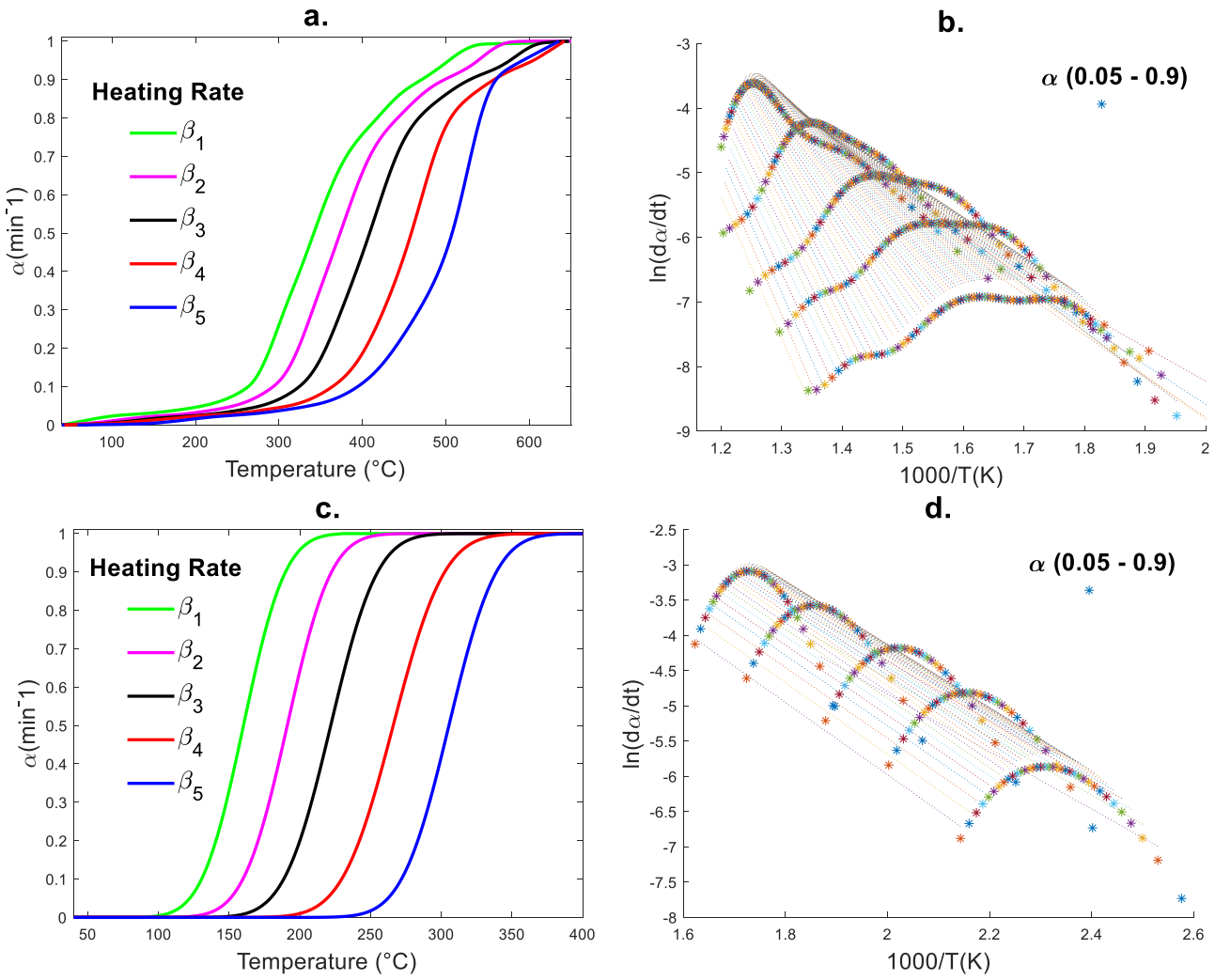

Figure 7. Friedman's method results for small particles in the air: conversion and slope of $\ln\left(\frac{d\alpha}{dt}\right)$ vs $1/T$ for the global analysis (a and b), and for peak 2 (c and d).

conditions where the most significant number of aromatic volatiles are generated and keeping them trapped within the solid is the key to proposing new process conditions.

On the other hand, knowing the volatiles that are lost in the gas phase during heating opens the doors to the possibility of proposing new designs of cocoa roasting equipment where it may be possible to trap these volatiles by condensation to be used for other applications in the pharmaceutical or cosmetic industry.

The heating also evidenced an effect on natural products such as methyalaxines theobromine and caffeine, which were found to be volatilized from 200 °C, increasing their concentration (related to the relative area) in the gas phase as the temperature increases. However, it was also identified that part of the theobromine remains inside the solid; that is, neither the heating nor the residence time were sufficient to volatilize these alkaloids. Theobromine is known to possess a bitter flavor present in cocoa roasted and chocolate products, and this alkaloid together with caffeine are found in relatively high concentrations in chocolate products.[47] Theobromine is important in the chocolate for its psychological effects associated with positive changes in human behavior, such as increased motivation/alertness and increased energy.[48] Besides, methylxanthines such as theobromine and caffeine contribute to chocolate cravings and preference for dark chocolate tastes and coffee.[49]

Kinetics. According to the results described above, the kinetic scheme of Figure 6 was proposed, where C is raw cacao, D is dry cacao, R is roasted cocoa, and O is over-roasted cocoa. The gas fraction contents W (vaporized water), V_1, and V_2 are the components volatilized after drying.

An example of results of α and slope of $\ln\left(\frac{d\alpha}{dt}\right)$ vs $1/T$ obtained by the Friedman model are presented in Figure 7 for both global and stage analysis. The E_a values of peaks are within the global distribution (Friedman and ASTM), as shown in Figure 8. Thus, the separate analysis is an appropriate methodology to better understand the nature of the roasting of cocoa particles.

Table 5 shows the E_a results for the maximum conversion slope given in Figure 7 ($\alpha = 0.5$). For each stage, the activation energy and pre-exponential factors tend to increase. The E_a values for L particles are slightly higher than for S; that is, a greater amount of energy is required to volatilize the gases, which may be a cause of the fact that as the larger particles the gases must have a longer way through the pores to exit the interior of the particle to the surface.

https://doi.org/10.1021/acsfoodscitech.1c00481
ACS Food Sci. Technol. 2022, 2, 1224−1236

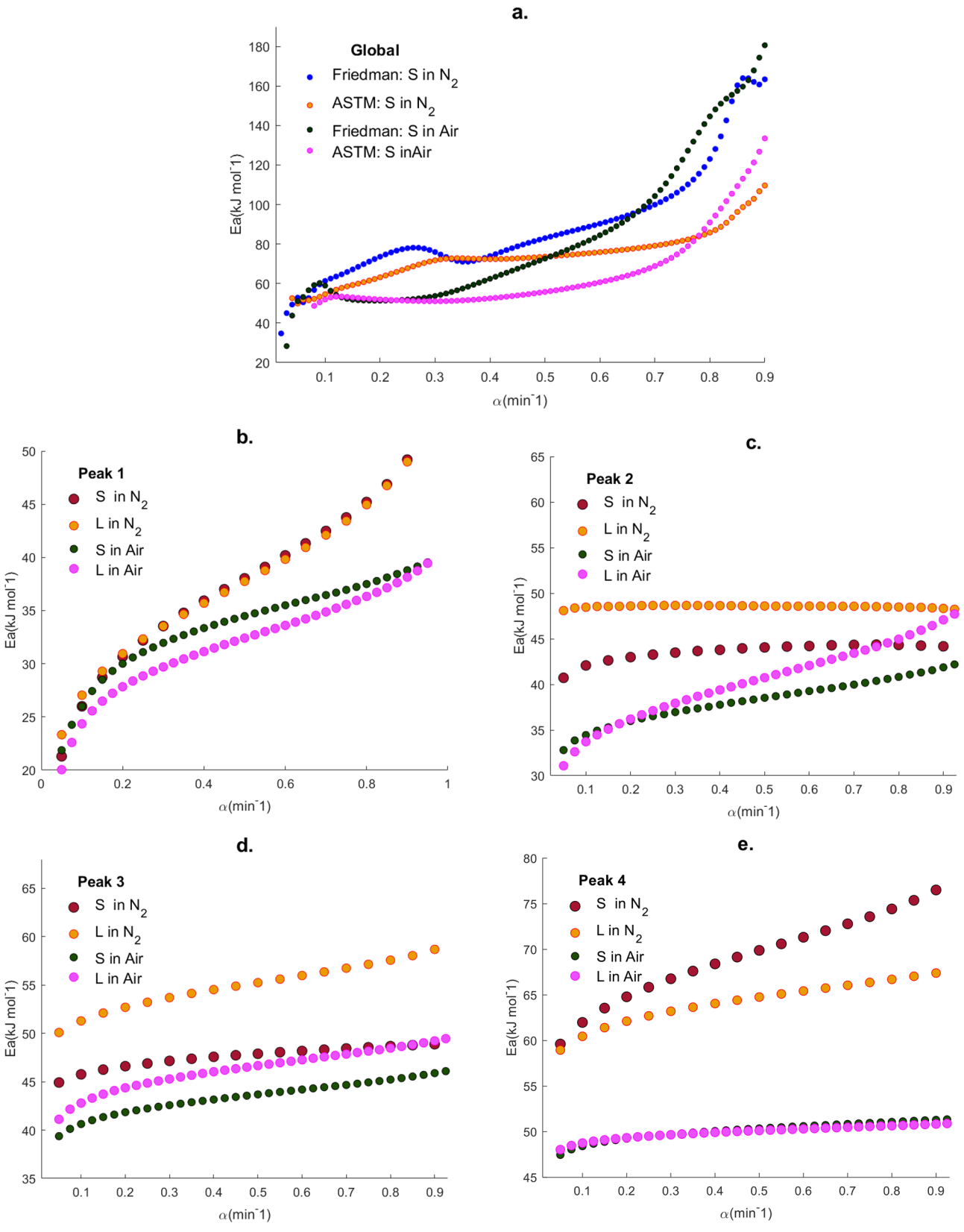

Figure 8. Distribution of activation energy (a) global by Friedman and ASTM method; by Friedman for (b) peak 1, (c) peak 2, (d) peak 3, and (e) peak 4.

The first peak, below 150 °C, is the drying of physisorbed water, volatile low molecular weight compounds, solvents and trapped gases in the solid.[50] The average of E_a for peak 1 was 32.7 kJ kmol^{-1}; this signal corresponds to the drying and volatilization of some low molecular weight compounds present in the raw cocoa. The E_a found is similar to the literature values (32.16 and 32.01 kJ mol^{-1}) for direct and indirect solar drying, as well as the signal of the evaporation of physisorbed water

https://doi.org/10.1021/acsfoodscitech.1c00481
ACS Food Sci. Technol. 2022, 2, 1224−1236

shown in the DTG curve up to 200 °C and the chemically bound water from 200 to 600 °C.[51] Initially, the E_a distribution of peak 1 does not show significant differences between N_2 and air (Figure 8b); that is, the process does not yet involve chemical reactions with oxygen, but a difference begins to appear with increasing temperature.

Peaks, 2, 3, and 4 of both S and L particles have lower E_a values for air (see Table 5 and Figure 8c−e). In other words, due to the interaction of oxygen with the surface of the particles, chemical oxidation reactions are generated, promoting volatilization. Similarly, to weight loss and DTG curves (not shown), in N_2 and air, of the TMP standard, pyrazines were volatilized from 150 to 300 °C, confirming that the pyrazines generated in the solid are volatilized in this range, and at 350 °C all the pyrazines can be volatilized to the gas phase.

Above 250 °C, there are peaks 3 and 4 where the decomposition reactions continue in cascade, generating many new volatiles within the solid that volatilize as they are generated, causing a large increase in reaction rate. The higher E_a values are determined (around 40 and 76 kJ mol^{-1}), because these reactions require more energy supplied by heat. Also, the differences between using N_2 or air are more evident, where the E_a values for air are lower than N_2, showing that oxygen is generating spontaneous reactions on the solid surface.

The global analysis by Friedman and ASTM showed comparable results (Figure 8*a*); therefore both methods are efficient in analyzing the conversion of cocoa during roasting. However, oxygen accelerated the conversion at 350 °C to 0.54 ± 0.0002 for S and 0.44 ± 0.02 for L, while nitrogen only reached 0.29 ± 0.0008 for S and 0.27 ± 0.003 for L particles.

E_a values have been found for several reaction models for browning, loss of amino acids, and formation of hydroxymethylfurfural (HMF) and pyrazine formation by Maillard reaction; however, these activation energies vary from 30 to 200 kJ mol^{-1}, depending on the conditions of the model experiment. Thus, the activation E_a obtained in this work, approximately between 10 and 140 kJ mol^{-2} (Friedman) and between 25 and 180 kJ mol^{-2} (ASTM), are within this wide range. Since the Maillard reaction is exceptionally complex and depends on several factors, the objective is to simplify the mechanism and try to identify the intermediate or final products of the reaction to understand which pathways are carried out during the heating of the cocoa particles.

CONCLUSIONS

The process of roasting cocoa particles was explained by three defined stages, starting with drying and continuing with the formation and transfer of volatiles to the gaseous phase, which is favored with slow heating. Furthermore, with the identification of volatiles generated, a new reaction network was proposed that includes degradation by oxidation since the results showed that oxygen affects the roasting process by accelerating the conversion. According to the main findings of this work, it is viable to design a roaster with inert gases and a condensation and recirculation system for gases to capture valuable volatile compounds.

AUTHOR INFORMATION

Corresponding Author

Farid Chejne − *Alliance for Biomass and Sustainability Research—ABISURE, Universidad Nacional de Colombia, Robledo, Medellín 0500034, Colombia;* orcid.org/0000-0003-0445-7609; Email: fchejne@unal.edu.co

Authors

Myriam Rojas − *Alliance for Biomass and Sustainability Research—ABISURE, Universidad Nacional de Colombia, Robledo, Medellín 0500034, Colombia; Department of Chemical Engineering, Engineering and Technology Institute Groningen, 9747 AG Groningen, The Netherlands; IN3 Corporation, Santa Ana, Pasto 520002, Colombia;* orcid.org/0000-0003-3081-2969

Jessi Osorio − *Department of Chemical Engineering, Engineering and Technology Institute Groningen, 9747 AG Groningen, The Netherlands*

Hero Jan Heeres − *Department of Chemical Engineering, Engineering and Technology Institute Groningen, 9747 AG Groningen, The Netherlands;* orcid.org/0000-0002-1249-543X

Complete contact information is available at: https://pubs.acs.org/10.1021/acsfoodscitech.1c00481

Notes

The authors declare no competing financial interest.
Data Availability Statement: Research data are shared.

ACKNOWLEDGMENTS

The authors would like to thank the ENgineering and TEchnology institute Groningen (ENTEG), the University of Groningen and Alliance for Biomass and Sustainability Research−ABISURE "Universidad Nacional de Colombia" Hermes code 5302, for supporting this work. Additionally, Farid Chejne wishes to thank the project "Strategy of the transformation of the Colombian energy sector in the horizon 2030" funded by call 788 of MINCIENCIAS. Contract no. FP44842-210-2018. Myriam Rojas would like to acknowledge the "Fundación CeiBA" for the Forgivable Education Grant for Ph.D. in Engineering. Jessi Osorio wishes to thanks the MINCIENCIAS for financial support with the educational grant no. 756-2016 for abroad Ph.D.

REFERENCES

(1) ICCO*The Chocolate Industry*; ICCO, 2019. https://www.icco.org/chocolate-industry/.

(2) Cambrai, A.; Marcic, C.; Morville, S.; Sae Houer, P.; Bindler, F.; Marchioni, E. Differentiation of Chocolates According to the Cocoa's Geographical Origin Using Chemometrics. *J. Agric. Food Chem.* **2010**, *58* (3), 1478−1483.

(3) Krysiak, W.; Adamski, R.; Zyzelewicz, D. Factors Affecting the Color of Roasted Cocoa Bean. *J. Food Quality* **2013**, *36* (1), 21−31. Redgwell, R. J.; Trovato, V.; Curti, D. Cocoa bean carbohydrates: roasting-induced changes and polymer interactions. *Food Chem.* **2003**, *80* (4), 511−516.

(4) Nanci, J.Chocolate Alchemy - Cocoa Bean Roasting. 2016. https://chocolatealchemy.com/cocoa-bean-roasting/ (accessed 2020-02-10).

(5) McCulloch, M.Cacao vs Cocoa: What's the Difference?. 2018. https://www.healthline.com/nutrition/cacao-vs-cocoa (accessed 2020-05-09).

(6) Adeyeye, E. I.; Akinyeye, R. O.; Ogunlade, I.; Olaofe, O.; Boluwade, J. O. Effect of farm and industrial processing on the amino acid profile of cocoa beans. *Food Chem.* **2010**, *118* (2), 357−363.

(7) (a) Barham, P.; Skibsted, L. H.; Bredie, W. L. P.; Bom Frøst, M.; Møller, P.; Risbo, J.; Snitkjær, P.; Mortensen, L. M. Molecular Gastronomy: A New Emerging Scientific Discipline. *Chem. Rev.* **2010**, *110* (4), 2313−2365. (b) Nursten, H. E.*The Maillard Reaction: Chemistry, Biochemistry, and Implications*; Royal Society of Chemistry, 2005.

(8) Aprotosoaie, A. C.; Luca, S. V.; Miron, A. Flavor chemistry of cocoa and cocoa products - an overview. *Comp. Rev. Food Sci. Food Safety* **2016**, *15* (1), 73−91.
(9) Afoakwa, E.; Paterson, A.; Fowler, M.; Ryan, A. Flavor formation and character in cocoa and chocolate: A critical review. *Crit. Rev. Food Sci. Nutrition* **2008**, *48* (9), 840−857.
(10) Castro-Alayo, E. M.; Idrogo-Vásquez, G.; Siche, R.; Cardenas-Toro, F. P. Formation of aromatic compounds precursors during fermentation of Criollo and Forastero cocoa. *Heliyon* **2019**, *5* (1), e01157.
(11) Araujo, Q. R.; Fernandes, C. A. F.; Ribeiro, D. O.; Efraim, P.; Steinmacher, D.; Lieberei, R.; Bastide, P.; Araujo, T. G. Cocoa Quality Index − A proposal. *Food Control* **2014**, *46*, 49−54.
(12) (a) Zzaman, W.; Bhat, R.; Yang, T. A. Effect of Superheated Steam Roasting on the Phenolic Antioxidant Properties of Cocoa Beans. *J. Food Process. Preserv.* **2014**, *38* (4), 1932−1938. (b) Stanley, T.Effects of alkalization and roasting on polyphenolic content of cocoa beans and cocoa powder. Master Thesis, The Pennsylvania State University, PA, 2014. (c) Gultekin-Ozguven, M.; Berktas, I.; Ozcelik, B. Change in stability of procyanidins, antioxidant capacity and in-vitro bioaccessibility during processing of cocoa powder from cocoa beans. *LWT-Food Sci. Technol.* **2016**, *72*, 559−565. (d) Misnawi; Jinap, S.; Jamilah, B.; Nazamid, S. Changes in polyphenol ability to produce astringency during roasting of cocoa liquor. *J. Sci. Food Agric.* **2005**, *85* (6), 917−924. (e) Ziegleder, G.Flavour development in cocoa and chocolate. In *Industrial Chocolate Manufacture and Use*, 4th ed.; Wiley-Blackwell, 2009; pp 169−191.
(13) Spizzirri, U. G.; Ieri, F.; Campo, M.; Paolino, D.; Restuccia, D.; Romani, A. Biogenic Amines, Phenolic, and Aroma-Related Compounds of Unroasted and Roasted Cocoa Beans with Different Origin. *Foods* **2019**, *8* (8), 306.
(14) Djikeng, F. T.; Teyomnou, W. T.; Tenyang, N.; Tiencheu, B.; Morfor, A. T.; Touko, B. A. H.; Houketchang, S. N.; Boungo, G. T.; Karuna, M. S. L.; Ngoufack, F. Z.; et al. Effect of traditional and oven roasting on the physicochemical properties of fermented cocoa beans. *Heliyon* **2018**, *4* (2), e00533.
(15) Oracz, J.; Nebesny, E. Effect of roasting parameters on the physicochemical characteristics of high-molecular-weight Maillard reaction products isolated from cocoa beans of different Theobroma cacao L. groups. *Eur. Food Res. Technol.* **2019**, *245* (1), 111−128.
(16) Mounjouenpou, P.; Belibi, D.; Andoseh, B. K.; Okouda, A.; Mouanfon, K.; Ehabe, E. E.; Ndjouenkeu, R. Temperature/duration couples variation of cocoa beans roasting on the quantity and quality properties of extracted cocoa butter. *Ann. Agric. Sci.* **2018**, *63* (1), 19−24.
(17) Del Rio, D.; Stewart, A. J.; Pellegrini, N. A review of recent studies on malondialdehyde as toxic molecule and biological marker of oxidative stress. *Nutrition, Metabolism and Cardiovascular Diseases* **2005**, *15* (4), 316−328.
(18) Jahurul, M. H. A.; Zaidul, I. S. M.; Norulaini, N. A. N.; Sahena, F.; Jinap, S.; Azmir, J.; Sharif, K. M.; Omar, A. K. M. Cocoa butter fats and possibilities of substitution in food products concerning cocoa varieties, alternative sources, extraction methods, composition, and characteristics. *J. Food Eng.* **2013**, *117* (4), 467−476.
(19) Rojas, M.; Chejne, F.; Ciro, H.; Montoya, J. Roasting impact on the chemical and physical structure of Criollo cocoa variety (Theobroma cacao L). *J. Food Process. Eng.* **2020**, *43*, e13400.
(20) Sandoval, A. J.; Barreiro, J. A. Water sorption isotherms of non-fermented cocoa beans (Theobroma cacao). *J. Food Eng.* **2002**, *51* (2), 119−123.
(21) Smith, K. W.19 - Confectionery Fats. In *Cocoa Butter and Related Compounds*; Garti, N., Widlak, N. R., Eds.; AOCS Press, 2012; pp 475−495.
(22) Talbot, G.1 - Chocolate and Cocoa Butter—Structure and Composition. In *Cocoa Butter and Related Compounds*; Garti, N., Widlak, N. R., Eds.; AOCS Press, 2012; pp 1−33.
(23) Tran, P. D.; Van de Walle, D.; De Clercq, N.; De Winne, A.; Kadow, D.; Lieberei, R.; Messens, K.; Tran, D. N.; Dewettinck, K.; Van Durme, J. Assessing cocoa aroma quality by multiple analytical approaches. *Food Res. Int.* **2015**, *77*, 657−669.
(24) Samaniego, I.; Espín, S.; Quiroz, J.; Ortiz, B.; Carrillo, W.; García-Viguera, C.; Mena, P. Effect of the growing area on the methylxanthines and flavan-3-ols content in cocoa beans from Ecuador. *J. Food Compos. Anal.* **2020**, *88*, 103448.
(25) Sacchetti, G.; Ioannone, F.; De Gregorio, M.; Di Mattia, C.; Serafini, M.; Mastrocola, D. Non enzymatic browning during cocoa roasting as affected by processing time and temperature. *J. Food Eng.* **2016**, *169*, 44−52.
(26) Beidaghy Dizaji, H.; Faraji Dizaji, F.; Bidabadi, M. Determining thermo-kinetic constants in order to classify explosivity of foodstuffs. *Combust., Explosion, Shock Waves* **2014**, *50* (4), 454−462.
(27) Domínguez-Pérez, L. A.; Concepción-Brindis, I.; Lagunes-Gálvez, L. M.; Barajas-Fernández, J.; Márquez-Rocha, F. J.; García-Alamilla, P. *Kinetic Studies and Moisture Diffusivity During Cocoa Bean Roasting* **2019**, *7* (10), 770.
(28) Baghdadi, Y. A.; Hii, C. l. Mass transfer kinetics and effective diffusivities during cocoa roasting. *J. Eng. Sci. Technol.* **2017**, *12* (1), 127−137.
(29) Hii, C. L.; Menon, A. S.; Chiang, C. L.; Sharif, S. Kinetics of hot air roasting of cocoa nibs and product quality. *J. Food Process Eng.* **2017**, *40*, e12467.
(30) Andruszkiewicz, P. J.; D'Souza, R. N.; Altun, I.; Corno, M.; Kuhnert, N. Thermally-induced formation of taste-active 2,5-diketopiperazines from short-chain peptide precursors in cocoa. *Food Res. Int.* **2019**, *121*, 217−228.
(31) Ioannone, F.; Di Mattia, C. D.; De Gregorio, M.; Sergi, M.; Serafini, M.; Sacchetti, G. Flavanols, proanthocyanidins and antioxidant activity changes during cocoa (Theobroma cacao L.) roasting as affected by temperature and time of processing. *Food Chem.* **2015**, *174*, 256−262.
(32) Pereira, A. P. M.; Stelari, H. A.; Carlin, F.; Sant'Ana, A. S. Inactivation kinetics of Bacillus cereus and Geobacillus stearothermophilus spores through roasting of cocoa beans and nibs. *LWT* **2019**, *111*, 394−400.
(33) Berčič, G. The universality of Friedman's isoconversional analysis results in a model-less prediction of thermodegradation profiles. *Thermochim. Acta* **2017**, *650*, 1−7.
(34) *E1641, A. Standard Test Method for Decomposition Kinetics by Thermogravimetry Using the Ozawa/Flynn/Wall Method*; ASTM International, 2018. DOI: 10.1520/E1641-18.
(35) (a) Font, R.; Garrido, M. A. Friedman and n-reaction order methods applied to pine needles and polyurethane thermal decompositions. *Thermochim. Acta* **2018**, *660*, 124−133. (b) Sobek, S.; Werle, S. Kinetic modelling of waste wood devolatilization during pyrolysis based on thermogravimetric data and solar pyrolysis reactor performance. *Fuel* **2020**, *261*, 116459. (c) Eseyin, A. E.; Steele, P. H.; Pittman, C. U.; Ekpenyong, K. I.; Soni, B. J. J. o. B. *TGA Torrefaction Kinetics of Cedar Wood* **2016**, *7*, 20−27. (d) Anca-Couce, A.; Tsekos, C.; Retschitzegger, S.; Zimbardi, F.; Funke, A.; Banks, S.; Kraia, T.; Marques, P.; Scharler, R.; de Jong, W.; et al. Biomass pyrolysis TGA assessment with an international round robin. *Fuel* **2020**, *276*, 118002. (e) Miranda, M. I. G.; Bica, C. I. D.; Nachtigall, S. M. B.; Rehman, N.; Rosa, S. M. L. Kinetical thermal degradation study of maize straw and soybean hull celluloses by simultaneous DSC−TGA and MDSC techniques. *Thermochim. Acta* **2013**, *565*, 65−71.
(36) Malvern. Mastersizer 3000. *Focus on Powder Coatings* **2012**, *2012* (1), 6.
(37) Abdilla-Santes, R. M.; Rasrendra, C. B.; Winkelman, J. G. M.; Heeres, H. J. Conversion of levoglucosan to glucose using an acidic heterogeneous Amberlyst 16 catalyst: Kinetics and packed bed measurements. *Chem. Eng. Res. Des.* **2019**, *152*, 193−200.
(38) O'Haver, T.*A Pragmatic Introduction to Signal Processing with applications in scientific measurement: An illustrated book with free software and spreadsheet templates to download*, 2020 ed.; Thomas O'Haver, 2020.
(39) Megías-Pérez, R.; Grimbs, S.; D'Souza, R. N.; Bernaert, H.; Kuhnert, N. Profiling, quantification and classification of cocoa beans

based on chemometric analysis of carbohydrates using hydrophilic interaction liquid chromatography coupled to mass spectrometry. *Food Chem.* **2018**, *258*, 284−294.
(40) Loureiro, G. A. H. A.; Araujo, Q. R.; Sodré, G. A.; Valle, R. R.; Souza, J. O.; Ramos, E. M. L. S.; Comerford, N. B.; Grierson, P. F. Cacao quality: Highlighting selected attributes. *Food Rev. Int.* **2017**, *33* (4), 382−405.
(41) (a) Krysiak, W. Effects of convective and microwave roasting on the physicochemical properties of cocoa beans and cocoa butter extracted from this material. *Grasas Aceites* **2011**, *62* (4), 467−478. (b) Oracz; Nebesny, E.; Żyżelewicz, D. Effect of roasting parameters on the physicochemical characteristics of high-molecular-weight Maillard reaction products isolated from cocoa beans of different Theobroma cacao L. groups. *Eur. Food Res. Technol.* **2019**, *245* (1), 111−128.
(42) Comesaña, R.; Gómez, M. A.; Álvarez, M. A.; Eguía, P. Thermal lag analysis on a simulated TGA-DSC device. *Thermochim. Acta* **2012**, *547*, 13−21.
(43) Ruan, D.; Wang, H.; Cheng, F.The Maillard Reaction. In *The Maillard Reaction in Food Chemistry: Current Technology and Applications*; Springer International Publishing, 2018; pp 1−21.
(44) (a) Counet, C.; Ouwerx, C.; Rosoux, D.; Collin, S. Relationship between procyanidin and flavor contents of cocoa liquors from different origins. *J. Agric. Food Chem.* **2004**, *52* (20), 6243−6249. (b) Saltini, R.; Akkerman, R.; Frosch, S. Optimizing chocolate production through traceability: A review of the influence of farming practices on cocoa bean quality. *Food Control* **2013**, *29* (1), 167−187.
(45) Zamora, R.; Hidalgo, F. J. *Maillard reaction and lipid oxidation* **2011**, *23* (3), 59−62.
(46) Hedegaard, R. V.; Skibsted, L. H.16 - Shelf-life of food powders. In *Handbook of Food Powders*; Bhandari, B., Bansal, N., Zhang, M., Schuck, P., Eds.; Woodhead Publishing, 2013; pp 409−434.
(47) (a) Stark, T.; Bareuther, S.; Hofmann, T. Molecular Definition of the Taste of Roasted Cocoa Nibs (Theobroma cacao) by Means of Quantitative Studies and Sensory Experiments. *J. Agric. Food Chem.* **2006**, *54* (15), 5530−5539. (b) Mitchell, E. S.; Slettenaar, M.; vd Meer, N.; Transler, C.; Jans, L.; Quadt, F.; Berry, M. Differential contributions of theobromine and caffeine on mood, psychomotor performance and blood pressure. *Physiol. Behavior* **2011**, *104* (5), 816−822.
(48) Yoneda, M.; Sugimoto, N.; Katakura, M.; Matsuzaki, K.; Tanigami, H.; Yachie, A.; Ohno-Shosaku, T.; Shido, O. Theobromine up-regulates cerebral brain-derived neurotrophic factor and facilitates motor learning in mice. *J. Nutrition. Biochem.* **2017**, *39*, 110−116.
(49) Smit, H. J.; Blackburn, R. J. Reinforcing effects of caffeine and theobromine as found in chocolate. *Psychopharmacology* **2005**, *181* (1), 101−106.
(50) Saadatkhah, N.; Carillo Garcia, A.; Ackermann, S.; Leclerc, P.; Latifi, M.; Samih, S.; Patience, G. S.; Chaouki, J. Experimental methods in chemical engineering: Thermogravimetric analysis—TGA. *Can. J. Chem. Eng.* **2020**, *98* (1), 34−43.
(51) Ameri, B.; Hanini, S.; Boumahdi, M. Influence of drying methods on the thermodynamic parameters, effective moisture diffusion and drying rate of wastewater sewage sludge. *Renew. Energy* **2020**, *147*, 1107−1119.

https://doi.org/10.1021/acsfoodscitech.1c00481
ACS Food Sci. Technol. 2022, 2, 1224−1236